Production of Ultrafine Grained Hardmetals by Electrical Resistance Sintering

Jesús Cintas [1] , **Raquel Astacio** [1], **Francisco G. Cuevas** [2,*] , **Juan Manuel Montes** [1],
Thomas Weissgaerber [3], **Miguel Ángel Lagos** [4] , **Yadir Torres** [1] **and José María Gallardo** [1]

[1] Department of Materials Science and Engineering, Escuela Técnica Superior de Ingeniería,
Universidad de Sevilla, Camino de los Descubrimientos s/n, 41092 Sevilla, Spain; jcintas@us.es (J.C.);
rastacio@us.es (R.A.); jmontes@us.es (J.M.M.); ytorres@us.es (Y.T.); josemar@us.es (J.M.G.)

[2] Department of Chemical Engineering, Physical Chemistry and Materials Science, Escuela Técnica Superior
de Ingeniería, Universidad de Huelva, Campus El Carmen, Avda. Tres de Marzo s/n, 21071 Huelva, Spain

[3] Fraunhofer Institute for Manufacturing Technology and Advanced Materials, Winterbergstrasse 28,
01277 Dresden, Germany; Thomas.Weissgaerber@ifam-dd.fraunhofer.de

[4] Tecnalia Research & Innovation, Mikeletegi Pasealekua 2, 20009 San Sebastián, Spain;
miguel.lagos@tecnalia.com

* Correspondence: fgcuevas@dqcm.uhu.es; Tel.: +34-959217448

check for updates

Abstract: In this work, powders of cemented ultrafine WC-6 wt.% Co were consolidated. The feasibility of the medium frequency electrical resistance sintering (MF-ERS) technique were studied to prevent WC grain growth during consolidation. Porosity and hardness were measured at different zones of the MF-ERS compacts. The compacts showed a slight inhomogeneity in their properties across their section, but it was controlled by choosing suitable values of the processing parameters. The optimal values for the material studied were current intensities between 7 and 8 kA and sintering times between 600 and 800 ms. The main achievement using this consolidation method was that sintered compacts essentially maintained the initial WC grain size. This was attained to processing times of less than 2 s, and without the need for using protective atmospheres.

1. Introduction

Conventional consolidation powder metallurgical (PM) techniques [1,2], mainly consisting of cold pressing and furnace sintering, are the most widely used, although the objective of finding a faster route has been a constant in researchers' mind.

New techniques are constantly emerging in an attempt to overcome the shortcomings of conventional processing. The direct use of electricity as a means to sinter powders has been suggested numerous times and with different approaches [3–11]. One of these techniques is electrical resistance sintering (ERS), in which heating is achieved by passing an electrical current through the powders.

The ERS process was already described in 1933 by Taylor [12] and later, in 1944, modified by Cremer [13], but its systematic study was not carried out until a few years later by Lenel [14]. Later, the ERS technique has incorporated technical variations of different importance [15,16]. Essentially, ERS involves the use of low voltage and high electrical current through a powder mass contained in an insulating die, while pressure is simultaneously applied. The medium frequency (about 1000 Hz) electrical resistance sintering (MF-ERS) technology has undergone an important evolution, making it possible to generate more heat for the same welding time.

The typical duration of the MF-ERS process is about one second. During this time, the applied current and pressure cause the densification of softened powders. This softening occurs by the

temperature increase caused by the current passing through the powders, and the energy released by the Joule effect.

Among the advantages of this technique, as compared to the conventional PM route, the following should be considered: the use of relatively low pressures (around 100 MPa) to reach high densification rates, the need for very short processing times, and the possibility of sintering in air, without protective atmospheres.

WC, used in the productions of hardmetals or cemented carbides, has a high hardness and a low ductility, so that pieces of this material are usually made from powders by adding between 6% and 10% of Co as a binding agent [17]. WC–Co is mainly used in the production of tools for milling, drilling, and pressing/punching processes, although it is also used in jewelry or to make surgical instruments. Very good properties are attained by maintaining the size of WC grain size in the limit of 1 to 5 μm, although limiting the size to 0.5 μm allows achieving a unique combination of properties.

This paper details the production of hardmetal parts by electrical resistance sintering. The main aim of this work was to study the effect of current intensity and sintering time on the properties and grain size reached in different zones of the produced compacts.

2. Materials and Methods

The starting material was a commercially ultrafine WC-6 wt.% Co powder from Kyocera Unimerco (Sunds, Denmark). WC-6 wt.% Co powder was degassed (840 °C/0.75 h/N_2H_2) to avoid problems due to gases expulsion during processing, and pre-sintered (1100 °C/2 h/Ar) in order to increase its particle size and facilitate further processing. The carbon and oxygen content was 5.78 and 0.13 wt.%, respectively. Figure 1 shows the achieved granulated powder where the WC particle size was 262 ± 77 nm. Mean particle size of this degassed and pre-sintered powder (WC6Co) was 141 μm (Figure 1c), as measured by laser diffraction in a Mastersizer 2000 (Malvern Panalytical, Malvern, UK).

| (a) | (b) | (c) |
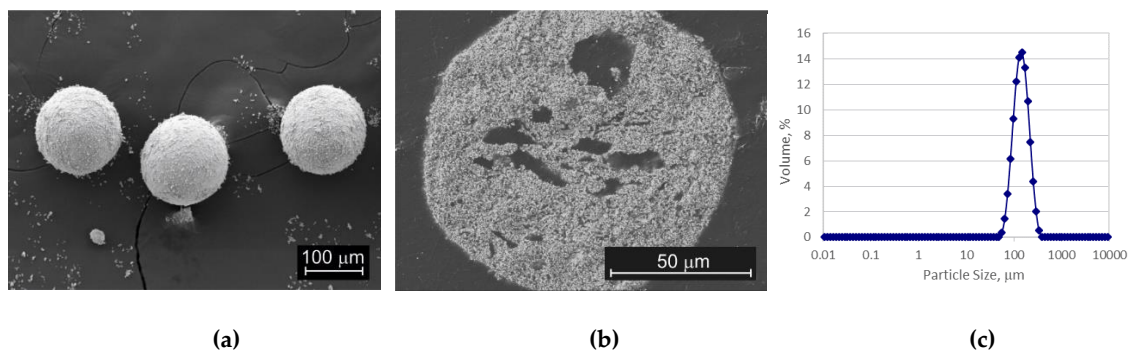
Figure 1. Degassed and pre-sintered WC-6 wt.% Co powder (WC6Co): Secondary electron SEM images of (**a**) the particles, (**b**) internal structure and (**c**) particle size distribution.

Compacts were prepared using a resistance welding machine (Beta 214 MF, Serra Soldadura, Barcelona, Spain), which was modified to implement the MF-ERS process. Figure 2a shows the scheme of the assembly used for MF-ERS, consisting of a 12 mm inner diameter ceramic tube (modified sodium zirconium phosphate-based ceramic, NZP) inserted in a metallic hoop. The powder mass (6.5 g in all experiences) was contained between two electrodes (thermal wafers and punches), all inside the ceramic tube. The temperature-resistant Cu electrodes (98.9% Cu, 1% Cr, 0.1% Zr) were in contact with heavy metal wafers (75.4% W, 24.6% Cu). These replaceable wafers were placed in direct contact with the powders to prevent electroerosion of the electrodes, powders sticking to the electrodes, and heat dissipation to the water-cooled electrodes due to their low thermal conductivity. In addition, to help the compacting process, the inner die wall was lubricated with a graphite–acetone suspension.
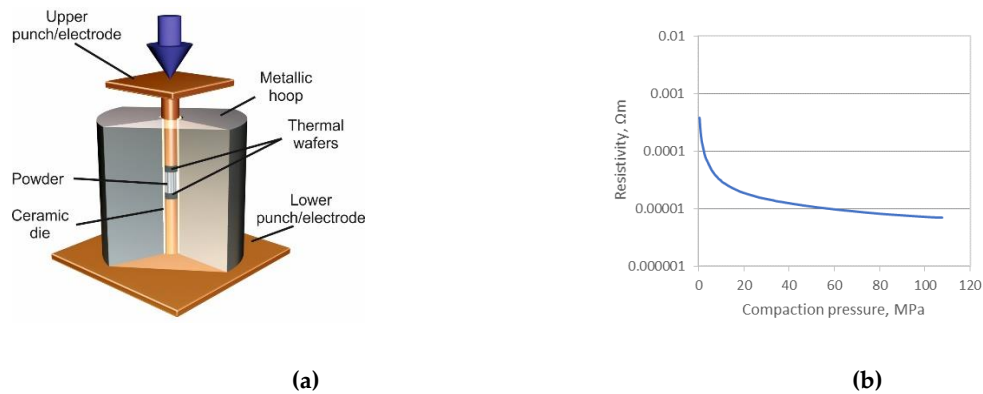
Figure 2. (**a**) Sketch of punches and die used in medium frequency electrical resistance sintering (MF-ERS) experiences, and (**b**) resistivity vs. compaction pressure of WC6Co powder.

The consolidation process consisted of three main stages: Cold pressing, sintering, and cooling. Compaction pressure, acting during the whole process, was 100 MPa for all the experiments. The cold-pressing and the cooling periods had a fixed duration of 1000 and 300 ms, respectively. The electrical current was only applied during the sintering stage. MF-ERS experiments were carried out with different current intensities and sintering times, always producing 12 mm diameter samples. Selected intensities were 6, 7, 8 and 9 kA, and heating times of 400, 600, 800 and 1000 ms were chosen. Intensities lower than 6 kA produced highly porous sintered samples. Intensities of 10 kA and above, combined with prolonged sintering times (1000 ms and longer), caused compacts welding to the wafers.

The previous description of the processing steps makes evident the importance of the relationship between the electrical resistivity and the compaction pressure, Figure 2b, because an adequate resistivity is required to allow the current passing at the time that causes the powders heating. Electrical resistance measurements were carried out by using a four-point probe with electrodes separated by 2 mm and a Kelvin bridge (micro-ohmmeter), by performing two measurements with inverted polarities to minimize the parasitic effects. Resistivity was determined from the measured resistance value. This powder showed a sharp drop in resistivity for low applied pressure values. The drop was lower as pressure increased. The resistivity values were between 3.76×10^{-4} and 6.87×10^{-6} Ωm in the range of 0 to 100 MPa.

Quantitative metallography on scanning electron microscopy (SEM) images (software Image Pro Plus 6, Media Cybernetics Inc., Rockville, MD, USA) was used to determine the porosity in specific regions of the compacts. The hardness of MF-ERS compacts was measured with a micro durometer Duramin-A300 (Struers GmbH, Willich, Germany), with the scale HV30, as recommended by the standard for hardmetals of this composition [18].

Samples were axially sectioned and subsequently prepared by appropriate grinding up to 400 grit SiC paper, and polishing on 6 and 3 μm diamond paste. Compact macrographs were taken with a D90 camera (Canon, Tokyo, Japan), and optical microscopy was performed with an EPIPHOT 200 microscope (Nikon, Tokyo, Japan). SEM studies of powders and compacts were carried out in a Dual Beam field emission gun scanning electron focused ion beam (FEGSEM-FIB) Auriga (Carl Zeiss, Oberkochen, Germany). In the case of sintered compacts, the same FEGSEM-FIB was required to resolve the exact morphology of these fine grained hardmetals. In order to improve the image quality, MF-ERS samples were, after being manually polished, ion etched into the microscope.

3. Results and Discussion

As compared to the relatively uniform porosity distribution in conventionally sintered compacts, MF-ERS compacts were characterized by a heterogeneous porosity distribution. Produced samples had a denser core than peripheral areas, as shown in Figure 3. This non-uniformity is the consequence of a

heterogeneous temperature distribution during processing, as shown by the process simulation [19]. In MF-ERS, the heating is produced by the Joule effect in the internal part of the sample. The temperature in the exterior is lower due to the heat transfer to the punches and die (the former are refrigerated and the latter acts as a heat sink). Therefore, MF-ERS compacts densify more in the inner, usually presenting the external porous layer (the brighter area) shown in Figure 3b.

(**a**)   (**b**)
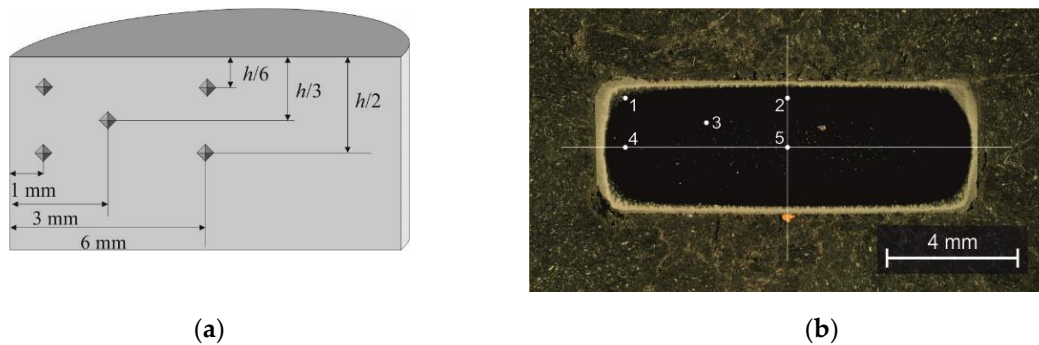
Figure 3. (**a**) Scheme and (**b**) metallographic section of a sintered sample showing the dot pattern where properties were studied.

In order to evaluate the homogeneity of the produced samples, properties at different zones of the specimen section have been studied. Taking into account the revolution symmetry of sintered compacts, a total of five zones distributed in a quadrant of an axial section of the compact were selected (Figure 3). In any case, measuring locations 1 to 5 were inside the zone limited by the porous outer layer surrounding the densified core of the specimen.

With the purpose of simplifying the graphical representation of the results, only the most representative zones (zones 1, 3 and 5) were shown. Zone 1 was chosen because it was located in the most extreme area of the compact, while zone 5 was in the center. Finally, zone 3 was at an intermediate distance from the previous ones.

Figure 4a shows the attained porosity, as a function of the current intensity, for 600 ms sintered compacts. As can be seen, the measured porosity values were always very low (less than 0.55 % and in general under 0.10 %). Even the porosity measured at zone 1, in the limit with the outer porous layer shown in Figure 3, was maintained at a very low value. Results reveal that the compact core (zone 5) was slightly more porous than the intermediate layer (zone 3). The reason for this was the air trapped inside the powder mass, which cannot be completely evacuated before closing the interconnected porosity, due to the very short sintering times. The porosity increases in zones 3 and 5 for the highest current intensity (9 kA) must be highlighted. The much quicker process under these circumstances accounts for this behavior.

Regarding the porosity evolution with sintering time (Figure 4b), a greater influence than with current intensity was observed. Increasing the sintering time increased the thermal transfer by Joule effect [20], causing the porosity to decrease as sintering time is extended. The same aforementioned phenomena of porosity increase for the most energetic conditions was observed for 1000 ms.

Therefore, it can be concluded that the best results, from the point of view of porosity, were achieved by sintering at not very high intensities (Figure 4a) and not very high heating times (Figure 4b), i.e., probably a good combination could result from 600 to 800 ms at 7 to 8 kA. These processing parameters also allowed a reduced outer porous layer, with a thickness lower than 100 μm. Mean density with the best conditions were therefore very near to that of commercial samples, around 14.75 g/cm^3 for the studied composition.

(**a**)　　　　　　　　　　　　　　　　　(**b**)
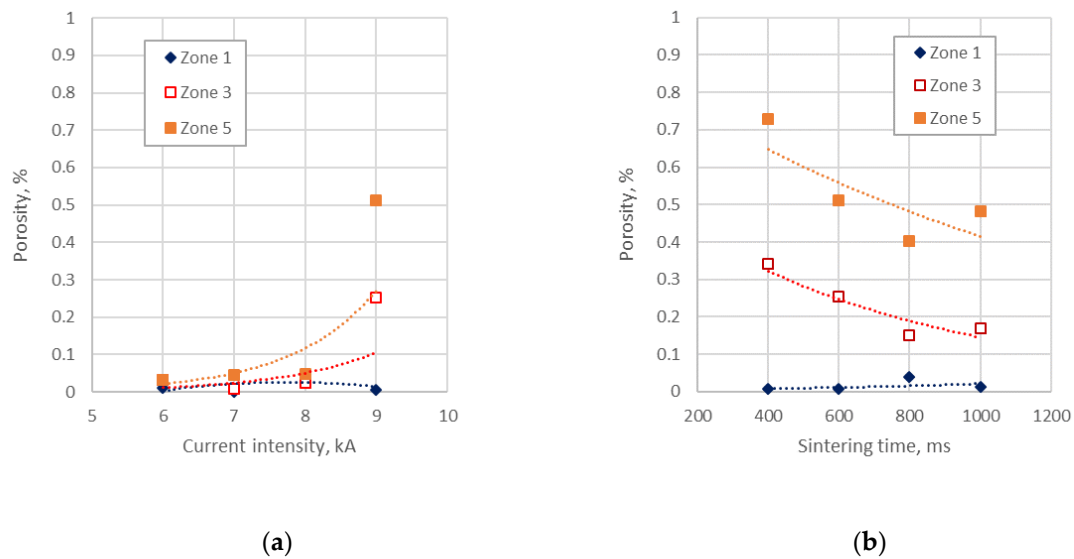
Figure 4. MF-ERS compacts porosity at zones 1, 3 and 5 as a function of (**a**) current intensity (experiences carried out at 600 ms), and (**b**) sintering time (experiences with 9 kA). Dotted lines are the trend lines of the different series.

In terms of hardness (Figure 5), most of the measured values are high, between 1800 and 2100 HV30. A typical value for commercial samples with this composition is around 1860 HV. The lowest values correspond to zones 3 and 5, according to the higher porosity at these zones, although possible different microstructural characteristics in both regions should also be considered.


(**a**)　　　　　　　　　　　　　　　　　(**b**)
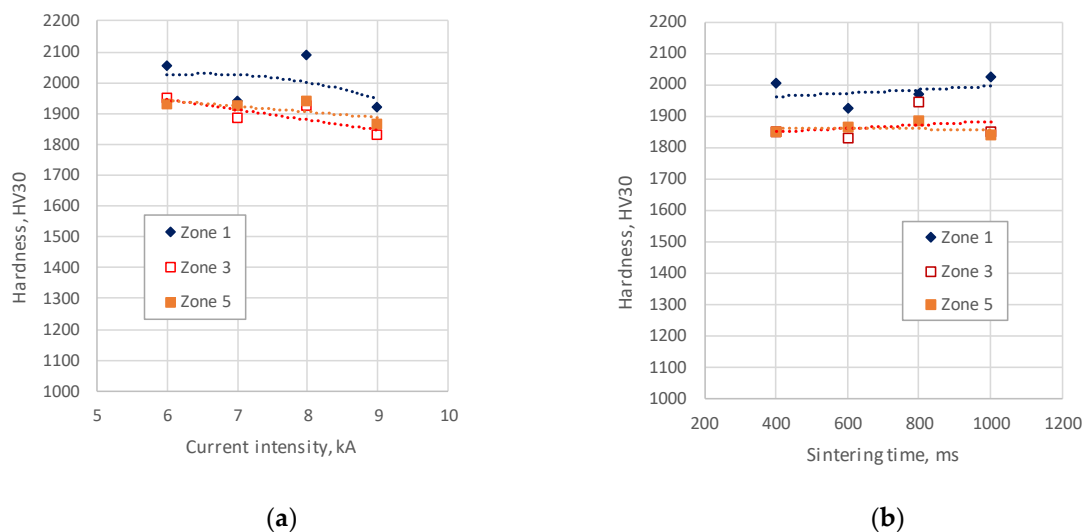
Figure 5. MF-ERS compacts hardness at zones 1, 3 and 5 as a function of (**a**) current intensity (experiences carried out with 600 ms), and (**b**) sintering time (experiences with 9 kA). Dotted lines are the trend lines of the different series.

The sintering conditions resulting in compacts with the best hardness values were between 600 and 800 ms, for intensities between 7 and 8 kA; that is, intervals coincident with those previously indicated for porosity.

Grain size is one of the most important factors in controlling materials properties. Mechanical strength, toughness, and hardness are important engineering properties that are strongly influenced by this parameter. For this reason, the tungsten carbide size distribution, along with Co interparticle free path, have been characterized in detail.

Measurement of carbide size was conducted according to the corresponding ISO standard [21]. As stated in the standard, a minimum of 200 grains of WC were measured to obtain a value as accurate as possible. This method was based on the average grain intercepts along a line across the material surface. In ultrafine grained hardmetals, as used in this study, the average grain size was so small that good quality images were difficult to obtain in conventional SEMs. However, it has been shown that a high resolution instrument which uses a field emission electron beam can provide acceptable images (Figure 6). The measurements of phase sizes were done after an ion etching (using the ion gun of the microscope) of the manually polished sample for improving the image quality.

(**a**)　　　　　　　　　　　　　　　　　(**b**)
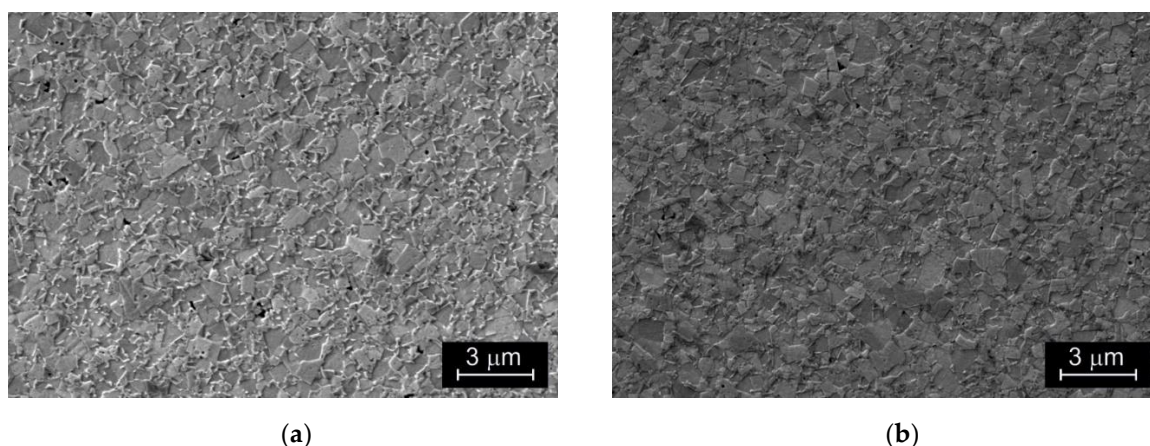
Figure 6. Secondary electron field emission gun SEM (FEGSEM) images of WC6Co compacts sintered at 9 kA–600 ms. Images correspond to positions (**a**) 3 and (**b**) 5 of the axial section of the compact.

Figure 6 shows representative FEGSEM images of the microstructure of a 9 kA–600 ms MF-ERS compact in zones 3 and 5. Similar images have been used for the full characterization of the carbides after the MF-ERS processes carried out with different processing conditions.

The results of WC grain size measurements are shown in Table 1. Only representative values from zones 3 and 5, of samples sintered for 600 ms are shown. Mean WC grain size slightly varied with sintering current intensity, ranging between about 260 and 325 nm, although not clearly modifying carbide sizes in a particular trend. The mean value for zone 3 results was 289 nm, whereas for zone 5 it was 297 nm. Carbide size distributions are very flat, with differences in general below the standard deviation for these measurements, which as shown in Table 1 are below 50 nm. In addition, due to the smaller size of Co regions as compared to WC, the accuracy of the measurements is lower, resulting in mean values about 39 nm for zone 3 and 49 nm for zone 5.

Table 1. Effect of current intensity on WC mean grain size and Co mean free path at zones 3 and 5, measured along a line perpendicular to the pressing direction. Sintering time was 600 ms.

|	Zone	Current Intensity, kA			
		6	7	8	9
WC Mean Size, nm	**3**	311 ± 45	267 ± 36	288 ± 31	289 ± 49
	5	258 ± 41	326 ± 25	287 ± 11	316 ± 28
Co Mean Free Path, nm	**3**	34 ± 4	37 ± 6	46 ± 9	38 ± 5
	5	49 ± 9	40 ± 8	53 ± 8	53 ± 7

Regarding the effect of sintering time, measurements on compacts sintered with a fixed current of 9 kA have been carried out (Table 2). WC mean size ranged between 273 and 327, with the Co mean free path between 37 and 60 nm for sintering times between 400 and 1000 ms. Again, there is not a clear effect of sintering time on microstructural features. Differences between both measuring zones and/or different sintering times were below the standard deviations for these measurements.

Table 2. Effect of sintering time on WC mean grain size and Co mean free path at zones 3 and 5, measured along a line perpendicular to the pressing direction. All samples were sintered at 9 kA.

	Zone	Sintering Time, ms			
		400	600	800	1000
WC Mean Size, nm	3	321 ± 52	289 ± 49	327 ± 49	309 ± 57
	5	273 ± 25	316 ± 28	301 ± 39	287 ± 20
Co Mean Free Path, nm	3	37 ± 4	38 ± 5	41 ± 5	52 ± 9
	5	60 ± 11	53 ± 7	58 ± 10	51 ± 7

In general, and comparing all the measured values, zone 5 showed slightly bigger grain sizes and Co mean free paths. As previously explained, the highest temperatures during MF-ERS processing were reached at zone 5, which could be consistent with the very slight increase in grain size observed.

It is also interesting to compare the WC grain size distributions in regions 3 and 5 of any particular sample. Figure 7 shows these values for the 7 KA–600 ms sintered compact. A higher percentage of small grains were measured at zone 3, although the minimum and maximum grain sizes were not so different. This was again in agreement with the highest temperature being reached at the core of the specimen.
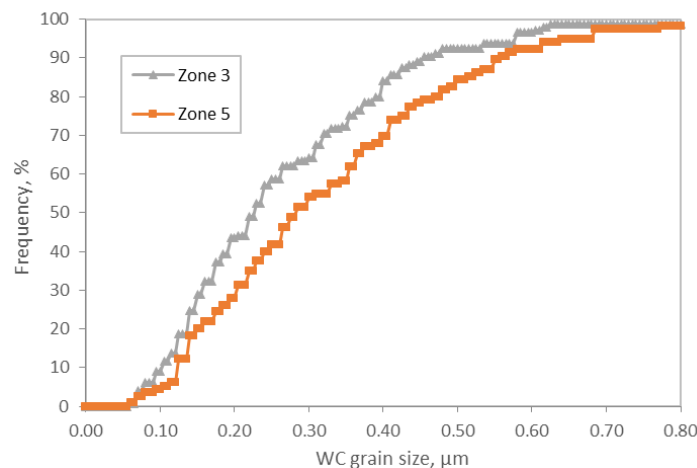
Figure 7. WC grain size distribution at zones 3 and 5 of compact sintered at 7 kA during 600 ms.

Regarding the effect on the WC grain size of the starting powder (262 ± 77 nm), it can be concluded that whichever the MF-ERS conditions, the WC grain size does not significantly grow during sintering. This is particularly important because using conventional hardmetals sintering methods, the WC grain size increased very quickly from the first few minutes of sintering [22]. In practice, to maintain such fine microstructures, grain growth inhibitors such as Cr_3C_2 or VC must be added in the material composition [23]. The proposed method of MF-ERS allows the ultrafine grain size of the WC powder to be maintained without using these additives. The high speed of the method is the key. This also brings another important aspect to highlight: there is no need to use protective atmospheres during sintering.

Finally, although out of the scope of this manuscript to be treated in detail, it is worth noting the toughness values reached in these materials. Palmqvist cracks induced from the corners of the Vickers indentation were related to the fracture toughness of the WC–Co [24]. Values show a certain anisotropy that can be eliminated through a heat treatment at 800 °C, reaching, for instance after processing at 7 kA and 800 ms, a mean value around 8.5 MPa·m$^{1/2}$.

4. Conclusions

In this work, ultrafine WC6Co powder was consolidated by MF-ERS. Results indicated that produced compacts were not completely homogeneous, with a slight variation of properties depending

on the zone of the specimen under consideration. Only a porous layer as thin as 100 μm was obtained in the outer surface of sintered samples.

Thus, for certain processing conditions (8 kA and 600 ms), porosity can be limited to values below 0.1%, regardless of the measuring zone of the cross section of the sample.

The hardness of sintered compacts was high, reaching for 8 kA and 600 ms values higher than 1900 HV30 at any zone of the sample.

It must be highlighted that the MF-ERS method has been proved perfectly suitable for producing, in less than two seconds, ultrafine hardmetals compacts with WC grain size in the order of the 300 nm, without the need for using a protective atmosphere.

Author Contributions: Conceptualization, J.M.G. and J.M.M.; methodology, J.C., F.G.C. and M.A.L.; validation, R.A., T.W. and Y.T.; writing—original draft preparation, J.C. and F.G.C.; writing—review and editing, all authors.

References

1. Cintas, J.; Montes, J.M.; Cuevas, F.G.; Gallardo, J.M. Influence of PCA content on mechanical properties of sintered MA aluminium. *Mater. Sci. Forum* **2006**, *514–516*, 1279–1283. [CrossRef]
2. Cintas, J.; Montes, J.M.; Cuevas, F.G.; Herrera, E.J. Influence of milling media on the microstructure and mechanical properties of mechanically milled and sintered aluminium. *J. Mater. Sci.* **2005**, *40*, 3911–3915. [CrossRef]
3. Grasso, S.; Sakka, Y.; Maizza, G. Electric current activated/assisted sintering (ECAS): A review of patents 1906–2008. *Sci. Technol. Adv. Mater.* **2009**, *10*, 1–24. [CrossRef] [PubMed]
4. Okazaki, K. Electro-discharge consolidation of particulate materials. *Rev. Part. Mater.* **1994**, *2*, 215–269.
5. Raichenko, A.I.; Chernikova, E.S. A mathematical model of electric heating of the porous medium using current-supplying electrode/punches. *Sov. Powder Metall. Met. Ceram.* **1989**, *28*, 365–371. [CrossRef]
6. Burenkov, G.L.; Raichenko, A.I.; Suraeva, A.M. Macroscopic mechanism of formation of interparticle contact in electric current sintering of powders. *Sov. Powder Metall. Met. Ceram.* **1989**, *28*, 186–191. [CrossRef]
7. Groza, J.R.; Zavaliangos, A. Sintering activation by external electrical field. *Mater. Sci. Eng. A* **2000**, *287*, 171–177. [CrossRef]
8. Wang, C.; Cheng, L.; Zhao, Z. FEM analysis of the temperature and stress distribution in spark plasma sintering: Modelling and experimental validation. *Comput. Mater. Sci.* **2010**, *49*, 351–362. [CrossRef]
9. Biesuz, M.; Pinter, L.; Saunders, T.; Reece, M.; Binner, J.; Sglavo, V.M.; Grasso, S. Investigation of electrochemical, optical and thermal effects during flash sintering of 8YSZ. *Materials* **2018**, *11*, 1214. [CrossRef] [PubMed]
10. Biesuz, M.; Dong, J.; Fu, S.; Liu, Y.; Zhang, H.; Zhu, D.; Hu, C.; Grasso, S. Thermally-insulated flash sintering. *Scr. Mater.* **2019**, *162*, 99–102. [CrossRef]
11. Biesuz, M.; Sglavo, V.M. Flash sintering of ceramics. *J. Eur. Ceram. Soc.* **2019**, *39*, 115–143. [CrossRef]
12. Taylor, G.F. Apparatus for Making Hardmetal Compositions. U.S. Patent 1,896,854A, 7 February 1933.
13. Cremer, G.D. Powder Metallurgy. U.S. Patent 2,355,954A, 15 August 1944.
14. Lenel, F.V. Resistance sintering under pressure. *Trans. AIME* **1955**, *7*, 158–167. [CrossRef]
15. Hara, Z.; Akechi, K. Electrical resistance sintering of titanium metal, alloys and composites. In *Titanium'80, Science and Technology, Proceedings of the 4th International Conference on Ti, Kyoto, Japan, 19–22 May 1980*; Kimura, H., Izumi, O., Eds.; The Metallurgical Society of AIME: New York, NY, USA, 1980; pp. 2265–2274.
16. Montes, J.M.; Rodríguez, J.A.; Cuevas, F.G.; Cintas, J. Consolidation by electrical resistance sintering of Ti powder. *J. Mater. Sci.* **2011**, *46*, 5197–5207. [CrossRef]

17. Pötschke, J.; Säuberlich, T.; Vornberger, A.; Meese-Marktscheffel, J.A. Solid state sintered nanoscaled hardmetals and their properties. *Int. J. Refract. Met. Hard Mater.* **2018**, *72*, 45–50. [CrossRef]

18. *Hardmetals: Vickers Hardness Test*; ISO 3878; ISO: Geneva, Switzerland, 1983.

19. Montes, J.M.; Cuevas, F.G.; Cintas, J.; Urban, P. A One-Dimensional Model of the Electrical Resistance Sintering Process. *Metall. Mater. Trans. A* **2015**, *46*, 963–980. [CrossRef]

20. Montes, J.M.; Cintas, J.; Cuevas, F.G.; Rodriguez, J.A. Electrical resistance sintering of M.A. Al-5AlN powders. *Mater. Sci. Forum* **2006**, *514–516*, 1225–1229. [CrossRef]

21. Hardmetals: Metallographic Determination of Microstructure. *Part 2: Measurement of WC Grain Size*; ISO 4499-2; ISO: Geneva, Switzerland, 2008.

22. Mannesson, K.; Elfwing, M.; Kusoffsky, A.; Norgren, S.; Ågren, J. Analysis of WC grain growth during sintering using electron backscatter diffraction and image analysis. *Int. J. Refract. Met. Hard Mater.* **2008**, *26*, 449–455. [CrossRef]

23. Pötschke, J.; Richter, V.; Gestrich, T.; Säuberlich, T.; Meese-Marktscheffel, J.A. Grain growth inhibition in ultrafine hardmetals. *Int. J. Refract. Met. Hard Mater.* **2017**, *66*, 95–104. [CrossRef]

24. Ponton, C.B.; Rawlings, R.D. Vickers indentation fracture toughness test, part 1: Review of literature and formulation of standardised indentation toughness equations. *Mater. Sci. Technol.* **1989**, *5*, 865–872. [CrossRef]